Available online at www.sciencedirect.com
SCIENCE DIRECT®
Polymer 44 (2003) 3333–3346
polymer
www.elsevier.com/locate/polymer

The influence of competitive interactions on multiple eutectic phase behavior in poly(ethylene oxide) molecular complexes

Laurence A. Belfiore*, Cynthia K.S. Lee, Jianguo Tang

Polymer Physics and Engineering Laboratory, Department of Chemical Engineering, Colorado State University, Fort Collins, CO 80523, USA

Received 18 September 2002; received in revised form 19 December 2002; accepted 8 January 2003

Dedicated to the memory of our friend and CSU colleague, Professor Rajiv Bhadra, who left us much too early on June 2nd, 2002. Our thoughts are with him, always.

Abstract

Binary mixtures of poly(ethylene oxide) and resorcinol exhibit two eutectic phase transitions at 40 and 80 °C, which are separated by a single-phase stoichiometric complex at ≈33 mol% resorcinol. These eutectic temperatures increase slightly at higher molecular weights of poly(ethylene oxide). The eutectics and the molecular complex are absent in ternary mixtures with either 25 or 40 wt% poly(2-vinylpyridine) because both polymers contain electron-pair donors which participate in hydrogen bonding interactions with the hydroxyl groups of the small-molecule aromatic. In contrast, 25 wt% polystyrene does not disrupt the bi-eutectic phase behavior of poly(ethylene oxide) and resorcinol because polystyrene is inert in these ternary mixtures. The lightest lanthanides with the largest ionic radii in the first-row of the f-block, like $LaCl_3(H_2O)_6$ and $CeCl_3(H_2O)_x$, are more effective than neodymium, terbium and ytterbium trichloride hexahydrates from the viewpoint of (i) competing with resorcinol, (ii) interacting with poly(ethylene oxide), (iii) eliminating eutectic melting, and (iv) disrupting the 2:1 stoichiometric complex between poly(ethylene oxide) and resorcinol. High-resolution ^{13}C solid state NMR spectroscopy identifies resorcinol in several different molecular environments. Multiple resonances are observed for chemically equivalent, but morphologically and crystallographically inequivalent, ^{13}C sites in the solid state. The isotropic chemical shift of the phenolic ^{13}C site in this small-molecule aromatic is very sensitive to the strength of intermolecular interactions in various phases. For example, self-association of resorcinol in pure crystalline phase γ yields a phenolic carbon chemical shift at 155 ppm. The formation of a 2:1 stoichiometric complex between poly(ethylene oxide) and resorcinol in co-crystallized phase β is identified by a phenolic carbon chemical shift at 158 ppm. When resorcinol and poly(2-vinylpyridine) interact in a homogeneous amorphous phase, the phenolic carbon resonance appears at a chemical shift of 160 ppm. A resorcinol-rich disordered crystalline phase in ternary mixtures with poly(ethylene oxide) and poly(2-vinylpyridine) yields a phenolic carbon resonance at 159 ppm. Temperature-composition projections of the binary and ternary phase diagrams, constructed via differential scanning calorimetry, allow one to interpret ^{13}C NMR spectra of these strongly interacting blends and complexes in the solid state.

Keywords: Poly(ethylene oxide); lanthanides; carbon-13 solid state NMR spectroscopy

1. Introduction

1.1. Previous studies of poly(ethylene oxide) molecular complexes

Mixing phenomena in macromolecular complexes are important from an engineering design viewpoint because miscibility considerations have a significant effect on bulk macroscopic physical properties [1]. At the site-specific level of probing interactions between dissimilar species in a mixture [2–5], one can identify functional groups that are responsible for exothermic energetics and the formation of a complex [6–8]. There are more than 500 publications in the research literature that focus on poly(ethylene oxide), PEO, complexes with lithium cations, and these complexes are useful for solid state battery applications [9]. Along these lines, it is well-known that metal salts increase the glass transition temperature of polyethers [10]. There are several examples (i.e. >20) of eutectic crystallization [11,12] in PEO molecular complexes [13–20], and even more solid state NMR studies of undiluted PEO (i.e. >40). However, there are very few solid state NMR investigations of PEO molecular complexes which exhibit single or multiple

* Corresponding author. Tel.: +1-970-491-5395; fax: +1-970-491-7369.
E-mail address: belfiore@engr.colostate.edu (L.A. Belfiore).

0032-3861/03/$ - see front matter © 2003 Elsevier Science Ltd. All rights reserved.
doi:10.1016/S0032-3861(03)00026-0

eutectic phase behavior [15–17,21,22]. Some of the design strategies for developing poly(ethylene oxide) molecular complexes are based on minimizing the differences between melting temperatures, crystal systems, unit cell dimensions, and rates of crystallization of the pure components so that complexation and co-crystallization will occur spontaneously via self-assembly. This study represents an extension of previous work in Belfiore's research group [15–17], where PEO molecular complexes with isomers and derivatives of dihydroxybenzenes were developed and characterized by calorimetry and ^{13}C solid state NMR spectroscopy. PEO and resorcinol exhibit two eutectic phase transitions [15,16] at 40 and 80 °C, with eutectic compositions near 10 and 50 mol% resorcinol, respectively. The temperature-composition projection of the phase diagram for binary mixtures of PEO and *p*-nitrophenol [18] exhibits a molecular complex at 60 mol% PEO which separates two eutectics at 42 and 95 °C, where the eutectic at 95 °C reveals characteristics of the crossover from eutectic to peritectic phase transitions. A comparison of the crystallographic parameters in Table 1 for PEO, resorcinol, and *p*-nitrophenol suggests that it is important to minimize differences between pure-component melting temperatures in these hydrogen-bonding binary mixtures to maximize the probability for multiple eutectic solidification due to spontaneous complexation in the crystalline phase.

1.2. Eutectic phase behavior

There is not an overwhelmingly large number of polymeric systems which exhibit eutectic crystallization and melting. Smith et al. [25–27] studied the eutectic solidification of binary mixtures such as polyethylene (or isotatic polypropylene) with 1,2,4,5-tetrachlorobenzene, and polyethylene with hexamethylbenzene. Wittmann and St John Manley [28] showed that eutectic phase transformations can occur in mixtures of a polymer and a crystalline monomer [i.e. poly(ε-caprolactone) or poly(ethylene oxide) with trioxane] which offer the possibility of producing polymer–polymer composites in situ after solid state polymerization of the monomer. Polymer–polymer blends also exhibit eutectic-type minima on the liquidus line in a temperature-composition projection of the phase diagram, which represents the solid–liquid analogue of minimum boiling heterogeneous azeotropes [29] for vapour–liquid equilibria. Hwang et al. [30,31] demonstrated that polyurethane model compounds containing monodisperse hard segments exhibit segmental compatibility and one eutectic phase transition in binary mixtures with selected polyether macroglycols. The eutectic phenomenon has also been reported in unblended copolyesters and copolyamides [32,33]. One of the most interesting ternary systems which exhibits single eutectic phase behavior is poly(ethylene), hexamethylbenzene, and adamantane [34]. These three components melt simultaneously at 117 °C in the following vol.% ratio; 63:24:13. Due to differences in the supercooling required for each component to solidify, they crystallize simultaneously at 89 °C in the following vol.% ratio; 68:21:11. Interestingly enough, all three binary subsystems of poly(ethylene), hexamethylbenzene and adamantane exhibit single eutectic phase behavior [34].

1.3. Temperature-composition projection of the binary phase diagram for poly(ethylene oxide) and resorcinol

The temperature-composition projection of the binary phase diagram for methanol-cast films of poly(ethylene oxide) and resorcinol is illustrated in Fig. 1. The amorphous phase of PEO was neglected in constructing this diagram. As mentioned in the Abstract, two solid–solid–liquid transformations are observed at 40 and 80 °C, corresponding to eutectic compositions near 10 and 50 mol% resorcinol, respectively. The upper-critical-solution-temperature-like phase behavior mapped out by the liquidus line represents a distinctive feature of systems that exhibit a stoichiometric complex separated by two eutectic phase transitions [35]. This 2:1 molecular complex near 33 mol% resorcinol is designated as phase β. Since material response times of macromolecular systems increase significantly at lower temperatures, solid polymers rarely achieve a state of thermodynamic equilibrium. Hence, the sluggishness of a material's viscoelastic response and its inability to rearrange conformationally or spatially on the time scale of typical

Table 1
Melting temperatures (T_m) and crystallographic unit cell parameters for poly(ethylene oxide) and small-molecule aromatics

	T_m (°C) measured[a]	Crystal system	Unit cell parameters			Unit cell volume[b] (Å)^3
			a (Å)	*b* (Å)	*c* (Å)	
Polymers [23]						
PEO	65	Monoclinic (7/2 helix)	8.1	13.0	19.5	1667
Aromatics [24]						
Resorcinol	118	Orthorhombic	10.5	9.6	5.7	569 (2.93)
p-Nitrophenol	115	Monoclinic	6.2	9.0	11.7	632 (2.64)

[a] Melting temperatures are calculated from the endothermic peak.
[b] Numbers in parentheses represent ratios of unit cell volumes (PEO/aromatic).

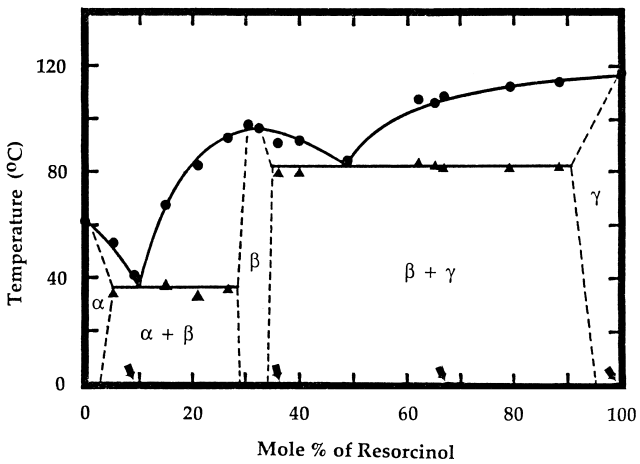

Fig. 1. Temperature-composition projection of the binary phase diagram for methanol-cast blends of poly(ethylene oxide), $\overline{M}_W = 3.4 \times 10^3$ Da, and resorcinol. Arrows on the horizontal axis identify mixtures whose NMR spectra are shown in Fig. 2. Reprinted with permission from Ref. [15].

experimental cooling rates yield a phase diagram in Fig. 1 that is representative of actual processing conditions. The PEO/resorcinol phase diagram resembles that of *p*-toluidine (i.e. *p*-aminotoluene) and phenol [12], in which eutectic compositions are observed at 30 and 75 mol% phenol, corresponding to phase transitions at 14 and 10 °C, respectively. A 1:1 stoichiometric complex separates the two eutectics and melts at 30 °C, which is lower than the pure-component melting temperatures of phenol (i.e. 40 °C) and *p*-toluidine (i.e. 42 °C) [12].

1.4. Spectroscopic detection of phase coexistence

Spectroscopic methods are sensitive to phase behavior when a signal from the 'key component' is influenced strongly by neighboring components in a complex. In some cases, a spectroscopic probe can detect phase coexistence when one of the phases is transparent to more conventional probes, like thermal analysis. For example, when the melting point depression phase boundary converges with the glass transition phase boundary as the crystallizable component is diluted by the noncrystalline component, thermal analysis might reveal only the dominant glass transition which overlaps a weak melting endotherm at the same temperature [3,6]. If the key component is present in the disordered crystalline and dominant amorphous phases, and if the interaction between dissimilar species is strong enough, then ^{13}C solid state NMR and, possibly, infrared spectroscopies will detect phase coexistence when the signal for the key component in each environment can be resolved. Hence, the overlap between T_g and T_m described above in amorphous/semicrystalline polymer–polymer blends is circumvented because the crystalline and amorphous regions are characterized by key component signals at different NMR chemical shifts and, possibly, different infrared vibrational frequencies. When eutectic phase behavior occurs, thermal analysis reveals one melting endotherm for a two-phase mixture at the eutectic composition. This is misleading because both phases that comprise the eutectic mixture melt incongruently [36,37] at the same temperature with no excess of either phase. In off-eutectic mixtures, the excess phase melts at higher temperature to produce a thermogram which reveals two endotherms. In both eutectic and off-eutectic mixtures of poly(ethylene oxide) with either resorcinol [15] or 2-methylresorcinol [17], carbon-13 solid state NMR spectroscopy detects phase-sensitive signals of the organic aromatic small molecule in each phase. Hence, the number of NMR absorptions for chemically indentical carbon sites in the resorcinol derivatives correlates with the number of coexisting phases. However, the number of crystalline phases in the solid state does not correlate with the number of DSC-measured melting endotherms at the eutectic composition.

1.5. Correlating high resolution ^{13}C solid state NMR spectra with the bi-eutectic phase behavior of poly(ethylene oxide) and resorcinol

Previous research in Belfiore's laboratory [3,4,16,38–41] revealed that strong intermolecular association in the solid state perturbs the ^{13}C isotropic chemical shifts of sites in the 'critical' component which exhibit sensitivity to the presence of dissimilar nearest neighbors. Examples of ^{13}C solid state NMR detection of microscopic mixing effects at ambient temperature are illustrated in Fig. 2 for three different mixtures of PEO and resorcinol. ^{13}C chemical shift assignments for resorcinol were made by adopting the substituent effects observed in solution for mono-substituted benzene compounds [42]. The aromatic carbon that is ortho to both hydroxyl groups appears between 100 and 110 ppm. The phenolic carbon signal is observed between 155 and 160 ppm. Some of the aromatic ^{13}C NMR signals of resorcinol in Fig. 2 are observed at different chemical shifts when PEO is present (spectra B–D) relative to undiluted resorcinol (spectrum 2A). For example, the phenolic carbon resonance at 155 ppm in undiluted resorcinol experiences a 3 ppm perturbation to larger chemical shift when resorcinol forms a stoichiometric hydrogen-bonded complex with PEO in phase β. This effect is indicated by the dashed line on the left side of Fig. 2. The aromatic carbon of resorcinol, which is located between the two hydroxyl groups, resonates at 103 ppm in the undiluted state (i.e. phase γ) and at 109 ppm in mixtures with PEO, as indicated by the dashed line and the arrow on the right side of Fig. 2. These three carbon sites in resorcinol are rather close to the macromolecular chain due to hydrogen bonding between the hydroxyl groups in the small molecule and the ether oxygen in PEO.

The 'off-eutectic' mixture whose overall composition is 67 mol% resorcinol lies in the middle of the β+γ two-phase region and exhibits two phenolic carbon resonances at 155 and 158 ppm. This is an example where ^{13}C solid state NMR

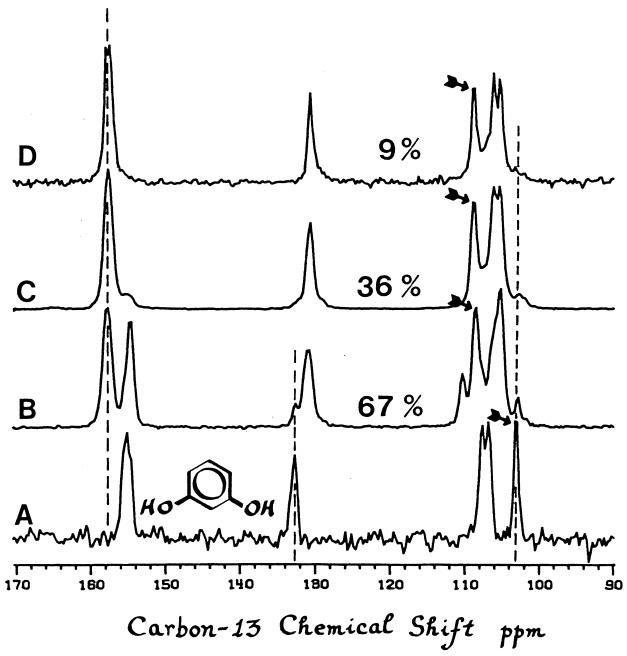

Fig. 2. High-resolution ^{13}C solid state NMR spectra of resorcinol and three methanol-cast blends with poly(ethylene oxide), $\overline{M}_W = 3.4 \times 10^3$ Da, focusing on the aromatic chemical shift region via cross-polarization with a contact time of 1 ms. (A) Undiluted crystalline resorcinol. (B) 67 mol% resorcinol. (C) 36 mol% resorcinol. (D) 9 mol% resorcinol. The pulse repetition delay was 60 s in spectrum (A), and 2 s otherwise. The dashed line on the left side identifies the chemical shift of the phenolic carbon of resorcinol in the molecular complex with PEO (i.e. phase β). The dashed line at ≈133 ppm identifies the aromatic carbon resonance in undiluted resorcinol that is meta to both hydroxyl substituents. This signal shifts to 131 ppm in complexes with PEO. The arrows and dashed line on the right side identify the aromatic resonance of resorcinol that is *ortho* to both hydroxyl groups. Reprinted with permission from Ref. [15].

spectroscopy identifies two different phases or molecular environments. One phase corresponds to the stoichiometric complex at 33 mol% resorcinol (i.e. phase β). The other phase, denoted by γ, is essentially 'NMR-indistinguishable' from undiluted resorcinol (i.e. spectrum 2A). In terms of the phenolic carbon resonance of resorcinol, phase β is observed at 158 ppm, and phase γ is observed at 155 ppm. Imashiro et al. [43,44] have reported specific examples where self-association via hydrogen bonding in the solid state is responsible for the fact that carbonyl ^{13}C resonances in various hydroxybenzaldehydes and enol forms of diketones appear at larger chemical shifts relative to their corresponding NMR spectra in solution. For bi-eutectic mixtures of PEO and resorcinol, intermolecular hydrogen bonding in the stoichiometric complex yields a phenolic carbon chemical shift which is larger than that in the self-associated resorcinol-rich phase. When the overall mixture composition is 36 mol% resorcinol, solid state NMR data reveal that phases β and γ are present at ambient temperature, but spectrum 2C and the 'lever rule' indicate that the stoichiometric complex (i.e. phase β at 158 ppm) is the dominant phase. Considering the quantitative constraints imposed by the cross-polarization pulse sequence for generating ^{13}C magnetization in the solid state, integrated intensities of the two phenolic carbon resonances in spectrum 2C seem to be qualitatively consistent with the lever principle in the two-phase region of the phase diagram. When the overall mixture composition lies to the left of the stoichiometric complex in the α + β two-phase region, spectrum D exhibits one phenolic carbon resonance at 158 ppm. This is consistent with the following facts; (i) the stoichiometric complex, denoted by phase β is present, (ii) resorcinol-rich phase γ is absent, and (iii) phase α is not detected because of the vanishingly small concentrations of resorcinol on the left side of the phase diagram in Fig. 1.

2. Experimental methods

2.1. Materials, and preparation of the complexes

Three different samples of poly-(ethylene oxide) were purchased from Scientific Polymer Products in Ontario, NY, with average molecular weights of 3.4×10^3, 2×10^5, and 9×10^5 Da, as indicated. No attempt was made to investigate the effect of PEO's molecular weight distribution on eutectic and liquidus phase transitions. Polystyrene ($\overline{M}_W = 2.34 \times 10^5$ Da) and poly(2-vinylpyridine) ($\overline{M}_W = 4 \times 10^4$ Da) were also purchased from Scientific Polymer Products. Resorcinol was obtained as a recrystallized white powder from Eastman Kodak Company in Rochester, NY. Lanthanum, cerium, neodymium, terbium, and ytterbium trichloride hydrates were purchased from Strem Chemicals in Newburyport, MA, with pure-component peak melting temperatures of 95, 97, 129, 169, and 162 °C, respectively, measured at a heating rate of 10 °C/min. All materials were used as received. Binary mixtures of poly(ethylene oxide) ($\overline{M}_W = 9 \times 10^5$ Da) and resorcinol were prepared from dilute methanol solutions (0.05 g solid/ml) at 35 °C. Upon evaporation of the solvent in a fume hood, solid residues were dried under vacuum at ambient temperature for approximately 12 h, followed by compression molding slightly above 120 °C for 3 min and subsequent cooling to room temperature. All films were dried further in a vacuum dessicator for 2 weeks at room temperature before physical characterization. Solid residues of low-molecular-weight PEO ($\overline{M}_W = 3.4 \times 10^3$ Da) and resorcinol were dried under vacuum at about 70 °C for comparable times (i.e. 15–20 h) without subsequent compression molding into films. Since resorcinol and PEO degrade at considerably different temperatures (i.e. 200 °C for resorcinol vs. 400 °C for PEO), thermogravimetric analysis of PEO/resorcinol residues was employed to calculate mixture compositions that were within 2% of the masses of the starting materials, prior to dissolution in methanol. An alternate route to prepare PEO molecular complexes relies on the fact that precipitation occurs when aqueous solutions of PEO and resorcinol are mixed. Thermogravimetric analysis of the recovered precipitates

Table 2
Reproducibility of thermal analysis data for poly(ethylene oxide), resorcinol, and either $LaCl_3(H_2O)_6$ or $TbCl_3(H_2O)_6$

Sample (composition in mol%)[a]	Storage time during vacuum desiccation (days)	Eutectic onset temp. (°C)	Eutectic peak temp. (°C)	Eutectic enthalpy (J/g)	Liquidus onset temp. (°C)	Liquidus peak temp. (°C)	Liquidus enthalpy (J/g)
Binary, 25% PEO, 75% Res	7	78	84	39	96	105	60
	20	79	84	37	97	105	59
Ternary, 25% PEO, 75% Res, 3.7% La	7	72	76	8	83	95	58
	20	66	72	8	85	90	62
Ternary, 25% PEO, 75% Res, 15% La	7				88	96	80
	20				88	94	93
Ternary, 25% PEO, 75% Res, 30% Tb	7	66	74	5	91	99	14
	20	62	72	6	91	99	18

[a] 3:1 molar ration of resorcinol to PEO. Ln^{3+} composition represents a molar ratio of the metal cation to the total moles of PEO and resorcinol.

after centrifugation revealed that all of them contain approximately 20–25 mol% resorcinol, independent of the composition of starting materials. These PEO/resorcinol precipitates are soluble in fresh water, in contrast to the water-insoluble high-molecular-weight complexes formed between PEO and poly(acrylic acid) [45]. Ternary mixtures of poly(ethylene oxide), resorcinol, and polystyrene were prepared from a 90/10 (v/v) cosolvent mixture of methylene chloride and methanol. Ternary mixtures of poly(ethylene oxide), resorcinol, and poly(2-vinylpyridine) were prepared from tetrahydrofuran. Ternary mixures of poly(ethylene oxide), resorcinol, and each of the lanthanide trichloride hydrates were prepared from methanol at 35 °C, dried under vacuum at 45 °C for 24–48 h, and desiccated at ambient temperature for one-to-three weeks prior to obtaining calorimetric data.

2.2. Thermal analysis

Differential scanning calorimetry of PEO/resorcinol mixtures was performed on a Perkin–Elmer DSC7. In most cases, thermograms were recorded at heating rates between 5 and 10 °C/min. In some cases, heating rates between 0.25 and 2 °C/min were employed to resolve eutectic and liquidus melting peaks near the eutectic composition. The effect of varying the heating rate between 0.25 and 5 °C/min produced an uncertainty of ± 1 °C in the endothermic peak temperature of both the indium standard and the polymeric complexes. Melting endotherms were measured during the first heating trace in the calorimeter. In this manner, phase diagrams constructed from these thermograms are not influenced appreciably by thermal history effects (other than ambient temperature annealing) and, most importantly, the kinetics of recrystallization. Following the suggestions of Etter et al. [36], and Gutt and Majumdar [37], eutectic and liquidus phase boundaries were constructed based on the following interpretation of DSC melting endotherms. When eutectic melting occurs, either in eutectic or off-eutectic mixtures, the peak temperature of the relatively sharp endotherm is used to construct an isothermal line representing three-phase solid–solid–liquid equilibrium. When melting occurs over a rather broad temperature range above the eutectic endotherm in off-eutectic mixtures, the endpoint of this broad asymmetric melting event is used to construct the liquidus line. When congruent melting occurs at local maxima on the liquidus line corresponding to pure components or the stoichiometric complex, the endpoint of the relatively sharp endothermic transition is chosen. The data in Table 2 illustrate reproducibility of thermal analysis results for eutectic and liquidus melting in selected binary and ternary mixtures.

2.3. Carbon-13 solid state NMR spectroscopy

Proton-enhanced dipolar-decoupled carbon-13 NMR spectra of binary and ternary mixtures in the solid state were obtained on a modified Nicolet NT-150 spectrometer in the Department of Chemistry at Colorado State University. The ^{13}C Larmour frequency was 37.735 MHz and magic-angle spinning was performed at 3600 Hz. The spectrometer contains a home-built cross-polarization/magic-angle spinning (CP/MAS) unit, including the probe. The spinner system is a modified version of Wind's [46] with a sample volume of 0.3 cm^3. A proton 90° pulse width of 5 μs was employed, corresponding to an rf field strength of 50 kHz. The rf field was maintained at 50 kHz during cross-polarization (i.e. 1 or 2 ms contact time during the Hartmann–Hahn match) and subsequent high-power ^1H decoupling. The ^{13}C free induction decay (FID) was accumulated in a 2K time-domain window using quadrature detection. Prior to Fourier transformation, the signal-averaged FID was zero-filled to 4K. The spectral width encompassed a ± 10 kHz frequency range and 5 Hz line broadening was employed. Spin-temperature alternation in the rotating frame was used to suppress the build-up of artifacts which may occur in proton-enhanced spectra [47]. The sample temperature was maintained at 15 °C ± 2 °C by passing the spinner air through a copper cooling coil immersed in an ice bath. Carbon-13 chemical shifts were referenced externally to the methyl resonance of hexamethylbenzene, 17.4 ppm deshielded from tetramethylsilane (i.e. TMS).

3. Results and discussion

3.1. Temperature-composition projection of the binary phase diagram for poly(2-vinylpyridine) and resorcinol

The melting point phase boundary for this interacting binary subsystem, illustrated in Fig. 3, was measured during the first DSC heating trace at a rate of 5 °C/min. Molten samples were cooled rapidly in the calorimeter, and the glass transition temperature was measured at a rate of 20 °C/min during the second heating trace. At high concentrations of resorcinol, one observes both T_g and T_m. The glass transition temperature of the amorphous phase exhibits an approximate linear relation with respect to blend composition, from ≈ − 25 °C for pure resorcinol to ≈92 °C for pure poly(2-vinylpyridine). Melting point depression of the resorcinol-rich phase is measured for mixtures which contain less than 35 wt% poly(2-vinylpyridine). This melting transition is progressively weaker and it occurs at lower temperatures which approach the increasing T_g of the amorphous phase at higher concentrations of poly (2-vinylpyridine). The absence of any appreciable supercooling range (i.e. $T_m - T_g$) at concentrations of poly (2-vinylpyridine) above 35 wt% is primarily responsible for the fact that crystallization of a resorcinol-rich phase does not occur. At 25 wt% poly(2-vinylpyridine), the DSC thermogram reveals both T_g and T_m, with an approximate 80 °C range of useful supercooling. At 40 wt% poly (2-vinylpyridine), the DSC trace reveals only a glass transition, which is near ambient temperature. These two binary mixture compositions are of interest because they represent the right-hand limit on binary projections of the ternary temperature-composition phase diagrams for poly(ethylene oxide) and resorcinol, with a constant amount of poly (2-vinylpyridine) (see Fig. 9 and 10). Hence, there is no melting point (i.e. liquidus) phase boundary when 40 wt% poly(2-vinylpyridine) is present and poly(ethylene oxide) is absent. Solid state ^{13}C NMR data in the following section provide conclusive evidence that no crystalline phase exists at 50 wt% poly(2-vinylpyridine), in binary mixtures with resorcinol.

3.2. ^{13}C solid state NMR spectra of binary mixtures containing poly(2-vinylpyridine) and resorcinol

Carbon-13 NMR data are presented in Fig. 4 between 100 and 170 ppm for undiluted poly(2-vinylpyridine) and two mixtures which contain 50 wt% and 75 wt% resorcinol. The ^{13}C solid state NMR spectrum of undiluted resorcinol was presented in Fig. 2(A). The upper spectrum in Fig. 4 at 75 wt% resorcinol corresponds to a two-phase semicrystalline mixture in which T_g is ≈5 °C and T_m is ≈90 °C. The resonances in the upper spectrum, which are relatively strong and narrow, correspond to a resorcinol-rich crystalline phase. The phenolic carbon signal appears at 155 ppm, similar to phase γ in Fig. 2, and two of resorcinol's three

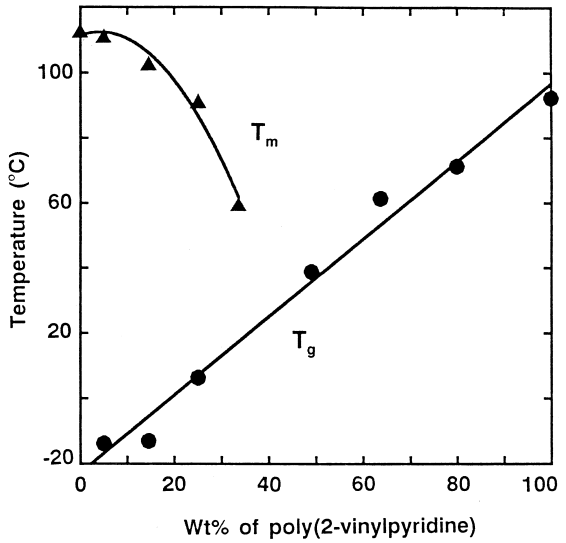

Fig. 3. Temperature-composition projection of the binary phase diagram for THF–cast mixtures of poly(2-vinylpyridine) and resorcinol. T_m was measured at a DSC heating rate of 5 °C/min. The glass transition temperature was measured at 20 °C/min after quenching molten samples in liquid nitrogen. Carbon-13 solid state NMR spectra are shown in Fig. 4 for mixtures that contain 25 and 50 wt% poly(2-vinylpyridine).

aromatic carbon signals between 100 and 110 ppm can be resolved. In the middle spectrum of Fig. 4, which corresponds to a completely amorphous mixture at 50 wt% resorcinol, all of the resonances are much broader with linewidths that resemble those of completely amorphous poly(2-vinylpyridine) in the lower spectrum. Since T_g of the 50 wt% resorcinol mixture is approximately 40 °C (i.e. see Fig. 3) and NMR experiments were performed at 15 °C, it is not unreasonable that the ^{13}C linewidths in the middle spectrum of Fig. 4 are characteristic of rigid glasses instead of highly viscous liquids. In the amorphous state, the phenolic carbon resonance of resorcinol appears at 160 ppm, as illustrated on the left side of both the middle spectrum and the upper spectrum in Fig. 4. It was difficult to determine if melting occurs in the mixture that contains 50 wt% resorcinol, but this DSC uncertainty is clarified via the middle spectrum of Fig. 4. There is no evidence of a phenolic carbon resonance at 155 ppm, due to a resorcinol-rich crystalline phase. The two resonances on the left side of the middle spectrum in Fig. 4 at 50 wt% resorcinol correspond to (i) the non-protonated aromatic ^{13}C signal of poly(2-vinylpyridine) at 164 ppm and (ii) the phenolic carbon of resorcinol at 160 ppm in a homogeneous amorphous phase. Hence, ^{13}C solid state NMR spectroscopy identifies the phenolic carbon resonance of resorcinol at (i) 155 ppm in undiluted or extremely resorcinol-rich crystalline phase γ, (ii) 158 ppm in a crystalline stoichiometric complex (i.e. phase β) with poly(ethylene oxide), and (iii) 160 ppm in a homogeneous amorphous mixture with poly(2-vinylpyridine). The chemical shifts of these morphologically inequivalent phenolic carbon sites are useful for phase behavior diagnostics of the small-molecule aromatic in crystalline and amorphous regions.

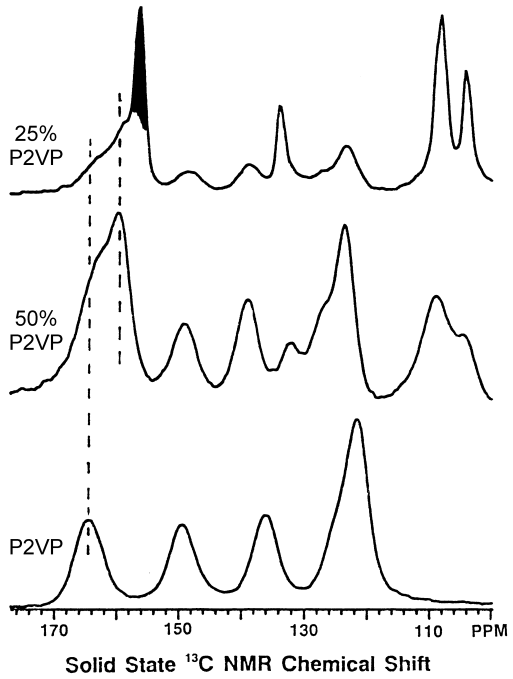

Fig. 4. High-resolution ^{13}C solid state NMR spectra of poly(2-vinylpyridine), P2VP, lower spectrum, and two THF–cast mixtures with resorcinol (i.e. middle spectrum, 50 wt% resorcinol; upper spectrum, 75 wt% resorcinol), focusing on the aromatic chemical shift region. The shaded resonance at 155 ppm identifies the phenolic carbon of resorcinol in crystalline phase γ. The dashed line at 160 ppm identifies the phenolic carbon resonance of resorcinol in a homogeneous amorphous phase with poly(2-vinylpyridine). The dashed line at 164 ppm identifies the non-protonated aromatic carbon of poly(2-vinylpyridine) that is bonded to the chain backbone.

3.3. Non-interacting binary subsystems; poly(ethylene oxide) with either poly(2-vinylpyridine) or polystyrene

These two non-interacting binary mixtures do not contain any functional group which interact specifically to yield exothermic energetics that are required for miscibility. For poly(ethylene oxide) and poly(2-vinylpyridine), the weak concentration dependence of the melting temperature and weight fraction of crystallinity, both of which are unique to the PEO-rich phase, is illustrated in Fig. 5. One observes T_m depression of 6 °C over a 90 wt% composition range, from pure PEO to 10 wt% PEO. For comparison, partially miscible blends of poly(ethylene oxide) with poly(vinylphenol) exhibit T_m depression of 15 °C over a 50 wt% composition range [3]. Fig. 5 also reveals that the crystalline weight fraction is not affected by poly(2-vinylpyridine) over a 45 wt% composition range, from pure PEO to 55 wt% PEO, when the experimental heat of fusion is based only on the mass of PEO in the blends. All of these trends are characteristic of very weakly interacting systems that are immiscible. The binary phase diagram for poly(ethylene oxide) and polystyrene is presented in Fig. 6, and it is very similar to the data in Fig. 5 for PEO and poly(2-vinylpyridine). Notice that the glass transition of the polystyrene-rich phase is approximately 30 °C higher than the melting transition of the PEO-rich phase. T_m depression of PEO in the presence of polystyrene is slightly less than 5 °C over a 90 wt% composition range in Fig. 6, from pure PEO to 10 wt% PEO. Previous studies of immiscible polymer blends containing completely amorphous polystyrene have reported (i) T_m depression of 3 °C at 40 wt% poly(vinylidene fluoride) [48], and (ii) between 2 and 6 °C T_m depression with semicrystalline polyolefins [49].

3.4. The persistence of bi-eutectic phase behavior in ternary mixtures of poly(ethylene oxide), resorcinol and polystyrene

The presence of 25 wt% polystyrene has an insignificant effect on the bi-eutectic phase behavior of PEO and resorcinol, as illustrated in Fig. 7. When the average molecular weight of PEO is 9×10^5 Da, and that of polystyrene is 2.34×10^5 Da, the eutectic solidification temperatures are 45 and 84 °C, with corresponding eutectic compositions near 10 and 50 mol% resorcinol, respectively. Based on a comparison with the phase diagram of Fig. 1, in which the PEO average molecular weight is 3.4×10^3 Da, these eutectic phase transitions occur at slightly higher temperatures when the molecular weight of PEO is larger. If the concentrations of these three components are presented on triangular coordinates and temperature is plotted vertically, then the eutectic and liquidus phase boundaries correspond to surfaces, which extend a significant distance away from the PEO/resorcinol edge of the three-dimensional phase diagram. The binary projection of the ternary phase diagram in Fig. 7 is extremely similar in appearance to the binary PEO/resorcinol phase diagram in Fig. 1, because there are no strong interactions between polystyrene and either PEO or resorcinol. Hence, polystyrene probably forms a separate amorphous phase whose glass transition is obscured by the liquidus phase boundary in Fig. 7

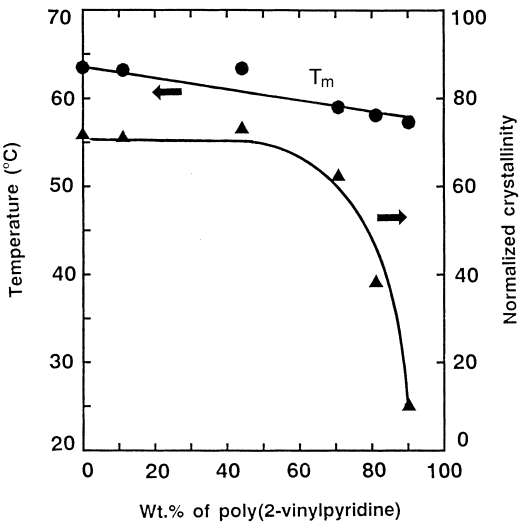

Fig. 5. Effect of poly(2-vinylpyridine) on the melting temperature and crystalline weight fraction of poly(ethylene oxide), $\overline{M}_W = 9 \times 10^5$ Da, in non-interacting polymer–polymer blends that were prepared from tetrahydrofuran. The melting temperature of PEO was recorded at a DSC heating rate of 10 °C/min.

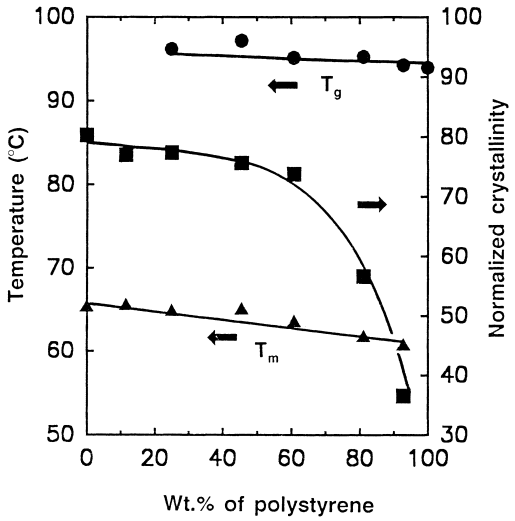

Fig. 6. Temperature-composition projection of the binary phase diagram for non-interacting immiscible polymer–polymer blends of poly(ethylene oxide), $\overline{M}_W = 9 \times 10^5$ Da, and polystyrene. The melting temperature of PEO and the glass transition temperature of the polystyrene-rich phase were measured at a DSC heating rate of 10 °C/min. The effect of polystyrene on the crystalline weight fraction of PEO is also included on the graph.

at high concentrations of resorcinol. It should be emphasized that the phase diagrams in Figs. 1 and 7 are 'similar in appearance', only, and the eutectics are essentially unperturbed by polystyrene. The ternary system in Fig. 7 contains an additional polystyrene-rich amorphous phase which is not present in binary mixtures of PEO and resorcinol. One concludes that polystyrene does not alter hydrogen bonding interactions between PEO and resorcinol, and their bi-eutectic phase behavior, as illustrated in Figs. 1 and 7, is preserved.

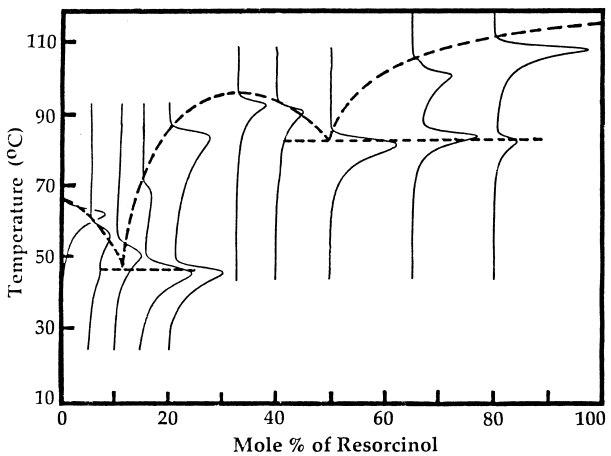

Fig. 7. Temperature-composition binary projection of the ternary phase diagram for poly(ethylene oxide), $\overline{M}_W = 9 \times 10^5$ Da, and resorcinol, illustrating bi-eutectic phase behavior in the presence of polystyrene which is almost identical to the binary phase diagram of PEO and resorcinol in Fig. 1. Actual thermograms are presented at 10 different mixture compositions on the phase diagram. These thermograms reveal either one or two melting events, and the connection between these melting transitions and the phase boundaries is illustrated by the dashed lines. All thermograms were recorded at a DSC heating rate of 5 °C/min. The mass fraction of polystyrene is 0.25 in each ternary mixture.

3.5. Effect of poly(2-vinylpyridine) on the bi-eutectic phase behavior of poly(ethylene oxide) and resorcinol

Five thermograms in Fig. 8 illustrate how poly(2-vinylpyridine) affects the eutectic and liquidus melting transitions of a 25/75 mol% off-eutectic mixture of poly(ethylene oxide) and resorcinol. When the concentration of poly(2-vinylpyridine) is 10 wt% or less, there is slight depression of the eutectic temperature and significant depression of the liquidus melting temperature. At 25 wt% and 40 wt% poly(2-vinylpyridine), eutectic melting is absent and the liquidus phase boundary, which has already been depressed by at least 15 °C, is essentially unaffected by the vinyl polymer. Complete binary projections of the ternary phase diagrams are illustrated in Fig. 9 at 25 wt% poly(2-vinylpyridine) and Fig. 10 at 40 wt% poly(2-vinylpyridine). In both cases, (i) eutectic melting is absent, (ii) melting point depression of the PEO-rich phase occurs on the left side of the diagrams, and (iii) melting point depression of the resorcinol-rich phase occurs on the right side of the diagrams. Hence, as one moves away from the PEO/resorcinol edge of the three-dimensional ternary phase diagram, the surface which represents the eutectic phase boundary at 84 °C disintegrates quickly, but the liquidus surfaces survive as long as PEO-rich and resorcinol-rich phases melt. Recall that the binary mixture of resorcinol and poly(2-vinylpyridine) which contains 40 wt% of the vinyl polymer reveals no melting behavior, as illustrated in Fig. 3. Hence, there is no liquidus boundary at the extreme right edge of the phase diagram in Fig. 10, but melting of a resorcinol-rich phase is observed when poly(ethylene oxide) is added to binary mixtures of resorcinol and poly(2-vinylpyridine). This morphological effect is a consequence of competitive interactions between resorcinol and both polymers which contain electron-pair donor groups. The hydroxyl group in resorcinol forms hydrogen bonds with the

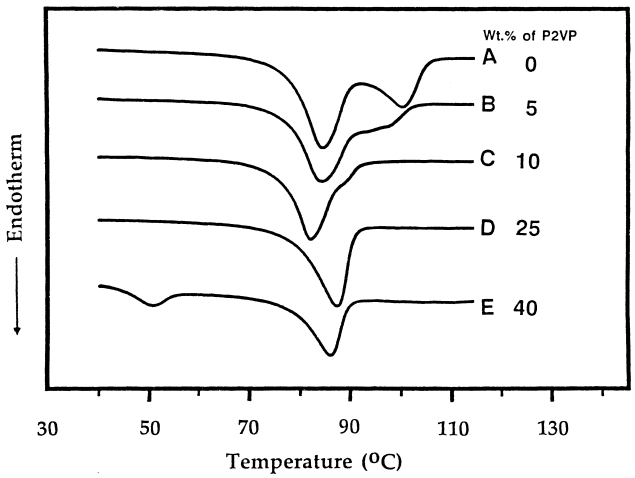

Fig. 8. DSC thermograms for ternary mixtures of poly(ethylene oxide), $\overline{M}_W = 9 \times 10^5$ Da, resorcinol, and poly(2-vinylpyridine). The PEO/resorcinol molar ratio is 1:3 in each ternary mixture, and the mass fraction of poly(2-vinylpyridine), P2VP, is indicated at the right of each thermogram.

(i) ether oxygen in PEO [16], and (ii) the pyridine nitrogen in poly(2-vinylpyridine). When the molar ratio of poly(ethylene oxide) and resorcinol is in the range of the stoichiometric complex (i.e. 2:1, or 33 mol% resorcinol), ternary mixtures which contain 25 wt% and 40 wt% poly(2-vinylpyridine) exhibit two melting endotherms that represent significant T_m depression of PEO-rich and resorcinol-rich phases. In this composition range (i.e. 20–35 mol% resorcinol with respect to PEO), the ternary mixtures contain two disordered crystalline phases and, at least, one amorphous phase. In fact, the endothermic event near 50 °C in thermogram E of Fig. 8 probably represents the glass transition of the amorphous phase which contains all of the poly(2-vinylpyridine) that is present, superimposed with 'T_g-overshoot' due to enthalpy relaxation in the vicinity of T_g. At lower concentrations of the vinyl polymer in Fig. 8, T_g is below 40 °C, and it was not detected in the DSC experiment.

3.6. ^{13}C solid state NMR spectra of ternary mixtures which contain poly(ethylene oxide), resorcinol and poly(2-vinylpyridine)

Carbon-13 solid state NMR spectra in the phenolic carbon chemical shift region are illustrated in Fig. 11 for undiluted poly(2-vinylpyridine) and four ternary mixtures in which resorcinol potentially interacts with both polymers, poly(ethylene oxide) and poly(2-vinylpyridine). When the mole fraction of resorcinol is between 0.25 and 0.90 with respect to poly(ethylene oxide), a resorcinol-like melting transition is observed between 60 and 90 °C in ternary mixtures which contain 40 wt% poly(2-vinylpyridine), as illustrated in Fig. 10. Ternary mixtures in this composition range exhibit a phenolic carbon resonance at 159 ppm due to this resorcinol-rich disordered crystalline phase in the

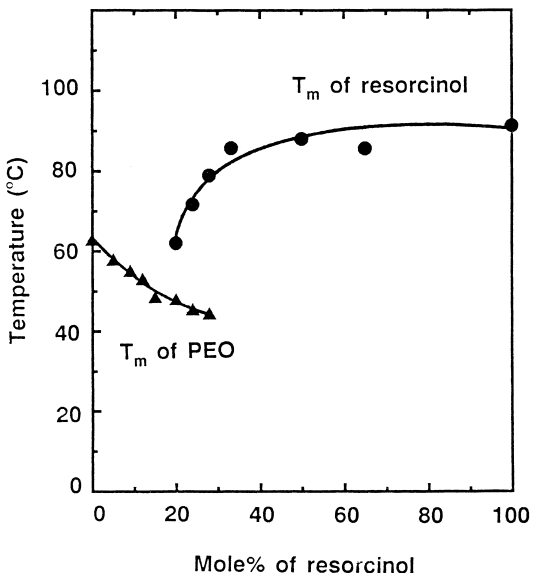

Fig. 9. Temperature-composition binary projection of the ternary phase diagram for poly(ethylene oxide), $\overline{M}_W = 9 \times 10^5$ Da, and resorcinol. The mass fraction of poly(2-vinylpyridine) is 0.25 in each ternary mixture.

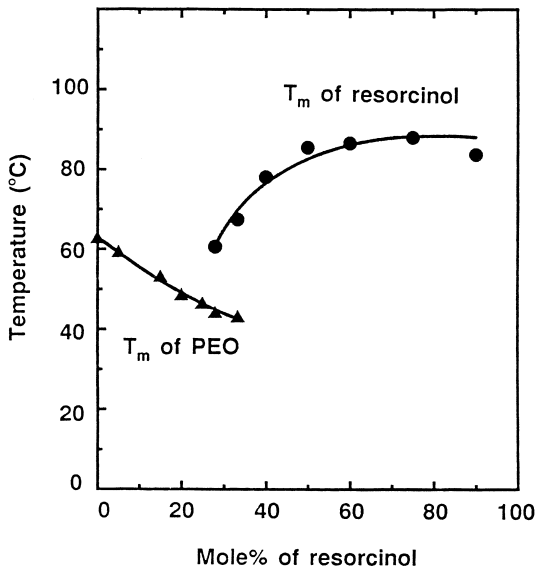

Fig. 10. Temperature-composition binary projection of the ternary phase diagram for poly(ethylene oxide), $\overline{M}_W = 9 \times 10^5$ Da, and resorcinol. The mass fraction of poly(2-vinylpyridine) is 0.40 in each ternary mixture.

presence of both polymers. This claim is justified by the upper two spectra in Fig. 11 at 33 mol% and 75 mol% resorcinol with respect to poly(ethylene oxide). When the mole fraction of resorcinol is 0.10 and 0.20 with respect to poly(ethylene oxide) in these ternary mixtures with 40 wt% poly(2-vinylpyridine), ^{13}C NMR spectra between 155 and 170 ppm in Fig. 11 identify the non-protonated aromatic carbon resonance of poly(2-vinylpyridine) at 164–165 ppm in the 2-position of the pyridine ring that is bonded to the chain backbone and the phenolic carbon resonance of resorcinol at 160–161 ppm (i.e. see the dashed line in Fig. 11). These ^{13}C resonances which are characteristic of a homogeneous amorphous phase. The PEO-rich crystalline phase does not contribute to this region of the NMR spectrum, and crystalline signals from resorcinol's phenolic carbon that have been detected at either 155, 158, or 159 ppm are absent. At 20 mol% resorcinol with respect to PEO, the phenolic carbon resonance at 159 ppm is absent in the middle spectrum in Fig. 11 because the liquidus boundary for the resorcinol-rich phase does not extend to 20 mol% resorcinol in Fig. 10. At 33 mol% resorcinol with respect to PEO, the NMR data in Fig. 11 suggest that a significant fraction of resorcinol resides in the amorphous phase because the strength of the ^{13}C signal at 160–161 ppm is comparable to that at 159 ppm, due to the resorcinol-rich disordered crystalline phase. At 75 mol% resorcinol with respect to PEO, the amorphous phenolic carbon resonance at 160–161 ppm is not resolved in the upper spectrum of Fig. 11, whereas the phenolic carbon resonance at 159 ppm for the resorcinol-rich disordered crystalline phase is dominant. In this case at 75 mol% resorcinol with respect to PEO, the melting temperature of the resorcinol-rich disordered crystalline phase (i.e. ≈90 °C) is depressed significantly from its pure-component

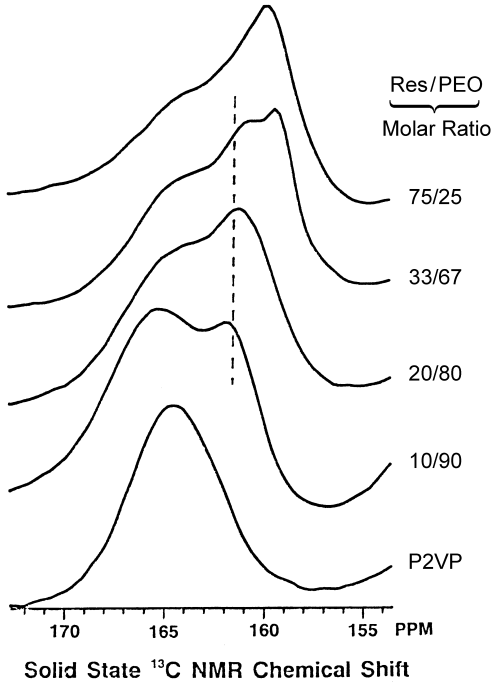

Fig. 11. High-resolution ^{13}C solid state NMR spectra of poly(2-vinylpyridine), P2VP, and four ternary mixtures with poly(ethylene oxide), $\overline{M}_W = 9 \times 10^5$ Da, and resorcinol in the phenolic carbon chemical shift region. The mass fraction of poly(2-vinylpyridine) is 0.40 in each ternary mixture, and the resorcinol/PEO molar ratio is indicated at the right of each spectrum. The dashed line identifies the phenolic carbon resonance of resorcinol in a homogeneous amorphous phase with poly(2-vinylpyridine).

T_m of 118 °C by poly(2-vinylpyridine), but not by poly(ethylene oxide). This claim is evident via inspection of the right side of the binary projection of the ternary temperature-composition phase diagram in Fig. 10, at 40 wt% poly(2-vinylpyridine).

3.7. Effect of lanthanide trichloride hydrates on the bi-eutectic phase behavior of poly(ethylene oxide) and resorcinol

There is only a handful of publications (i.e. ≈9) which focus on lanthanide complexes with poly(ethylene oxide) [50–58]. PEO forms amorphous complexes [53,57,58] with La^{3+}, Nd^{3+} and Eu^{3+} via displacement of lattice waters [51,58] by the ether group in the polymer. In some cases [58], the original anions (i.e. picrate) remain in the first shell coordination sphere when Eu^{3+} forms a complex with PEO. In other cases [54,55], eutectic solidification is reported near 60 °C in PEO complexes with Pr^{3+}, Nd^{3+} and Eu^{3+}, when the lanthanide cation mole fraction is between 0.059 and 0.125. However, these interpretations of eutectic phase behavior are somewhat tenuous, based on the thermograms that were presented. In a parallel study [59] of PEO complexes with several lanthanide trichloride hydrates (i.e. La^{3+}, Ce^{3+}, Eu^{3+}, Tb^{3+} and Yb^{3+}), there is no evidence of eutectic solidification in the temperature-composition projection of each binary phase diagram. Nevertheless, the potential exists to develop lanthanide complexes with polyethers, based on the fact that lanthanide cations have an affinity for oxygen, and the most stable lanthanide complexes contain chelating oxygen ligands [60]. Ternary PEO/resorcinol/lanthanide complexes are investigated from the viewpoint of competitive interactions. Hydrogen bonds form between PEO and resorcinol [15,16], whereas ion-dipole interactions [61] occur between PEO and the lanthanides. Five DSC thermograms in Fig. 12 illustrate how increasing concentrations of terbium trichloride hexahydrate affect the eutectic and liquidus melting endotherms of a 25/75 (mol/mol) off-eutectic mixture of poly(ethylene oxide) and resorcinol. Both endothermic peak temperatures decrease by approximately 10 °C immediately, upon introduction of the terbium complex in these ternary mixtures. However, the PEO/resorcinol eutectic melting transition survives in the presence of 30 mol% Tb^{3+}, and there is no gradual depression of the liquidus phase boundary, which represents melting of the resorcinol-rich phase. There is a significant difference between the effects of poly(2-vinylpyridine) and $TbCl_3(H_2O)_6$ on the liquidus melting endotherms, as illustrated in Figs. 8 and 12, respectively. In Fig. 8, increasing concentrations of poly(2-vinylpyridine) induce significant depression of the liquidus phase transition until it converges on the eutectic endotherm near 85 °C. In Fig. 12, the liquidus phase transition is depressed by 6–12 °C in the presence of terbium(III), but higher concentrations of the lanthanide do not induce a continuous decrease in the liquidus melting temperature. The effects of increasing concentrations of $NdCl_3(H_2O)_6$ and $YbCl_3(H_2O)_6$ on eutectic and liquidus melting of the same 25/75 (mol/mol) off-eutectic mixture of poly(ethylene oxide) and resorcinol in Figs. 13 and 14, respectively, are very similar to the effect of $TbCl_3(H_2O)_6$ in Fig. 12. The PEO/resorcinol eutectic phase transition at 84 °C decreases by approximately (i) 10 °C in the presence of Tb^{3+} and Yb^{3+}, and (ii) 20 °C in the presence of Nd^{3+}, when the lanthanide salt concentration is between 4 and 30 mol%. Liquidus melting is broadened significantly at 30 mol% Nd^{3+} and 15 mol% Yb^{3+}, but eutectic melting is not eliminated for Nd^{3+}, Tb^{3+}, and Yb^{3+} concentrations up to 30 mol%. The pure-component melting endotherms [62] of the following hexahydrates: terbium chloride (i.e. $T_m = 169$ °C), neodymium chloride (i.e. $T_m = 129$ °C), and ytterbium chloride (i.e. $T_m = 162$ °C), do not overlap any of the endothermic events between 50 and 120 °C in Figs. 12–14. Any controversy between melting vs. decomposition of these lanthanide complexes is addressed by the following facts and experimental observations. The formation of oxochlorides from lanthanide trichloride hydrates requires several hours above 200 °C [60]. For example, under mild conditions and rather short times near 120 °C in the calorimeter, both $LaCl_3(H_2O)_6$ and $CeCl_3(H_2O)_x$ melt in the vicinity of 95 °C during the first heating trace at a rate of 10 °C/min, and recrystallize during the subsequent cooling trace. This heating/cooling cycle was repeated to demonstrate reversibility of the melting and

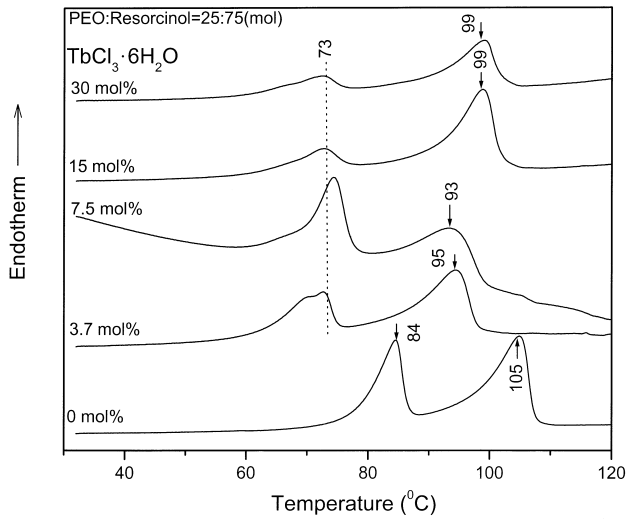

Fig. 12. DSC thermograms for ternary mixtures of poly(ethylene oxide), $\overline{M}_W = 2 \times 10^5$ Da, resorcinol, and terbium trichloride hexahydrate at a heating rate of 10 °C/min. The PEO/resorcinol molar ratio is 1:3 in each case, and the mole fraction of the low-molecular-weight lanthanide complex is indicated at the left of each thermogram. The dashed line at 73 °C identifies eutectic melting in all ternary mixtures which contain $TbCl_3(H_2O)_6$.

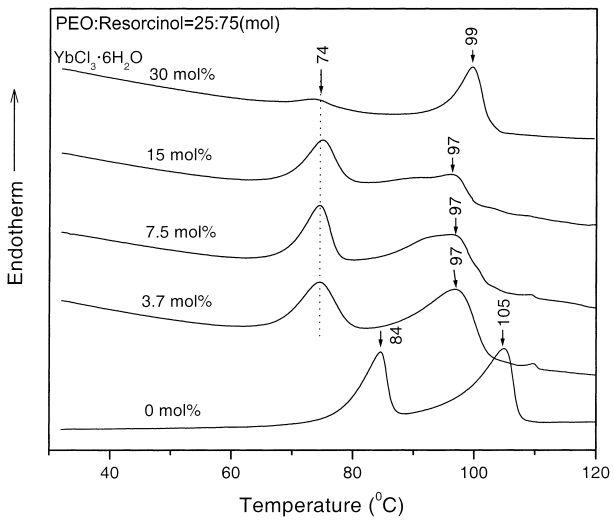

Fig. 14. DSC thermograms for ternary mixtures of poly(ethylene oxide), $\overline{M}_W = 2 \times 10^5$ Da, resorcinol, and ytterbium trichloride hexahydrate at a heating rate of 10 °C/min. The PEO/resorcinol molar ratio is 1:3 in each case, and the mole fraction of the low-molecular-weight lanthanide complex is indicated at the left of each thermogram. The dashed line at 74 °C identifies eutectic melting in all ternary mixtures which contain $YbCl_3(H_2O)_6$.

crystallization processes, and discard the possibility that thermal decomposition or the formation of oxochlorides occurs in these lanthanide complexes below 120 °C. Loss of a few lattice waters might be responsible for the fact that $LaCl_3(H_2O)_6$ melts at a significantly lower temperature during the second heating trace (i.e. 73 °C vs. 96 °C), but the irreversible production of oxides or oxochlorides during the first heating should eliminate melting and recrystallization

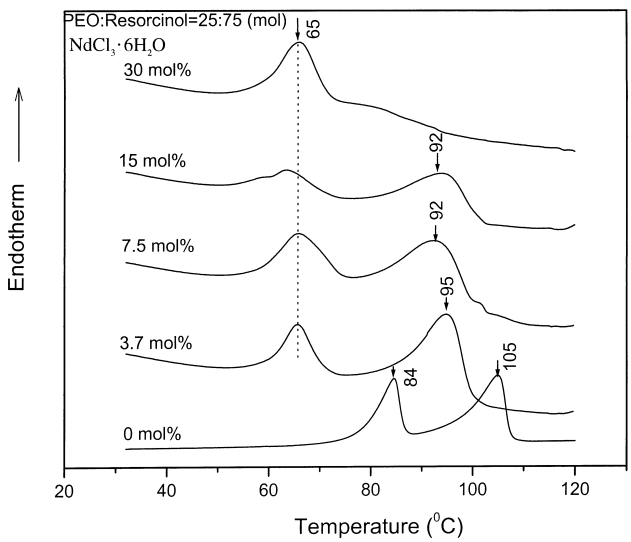

Fig. 13. DSC thermograms for ternary mixtures of poly(ethylene oxide), $\overline{M}_W = 2 \times 10^5$ Da, resorcinol, and neodymium trichloride hexahydrate at a heating rate of 10 °C/min. The PEO/resorcinol molar ratio is 1:3 in each case, and the mole fraction of the low-molecular-weight lanthanide complex is indicated at the left of each thermogram. The dashed line at 65 °C identifies eutectic melting in all ternary mixtures which contain $NdCl_3(H_2O)_6$.

during subsequent heating and cooling cycles. In contrast to the effects of Tb^{3+}, Nd^{3+} and Yb^{3+} on eutectic and liquidus melting of PEO and resorcinol, 15 mol% lanthanum trichloride hexahydrate completely eliminates eutectic melting in a 25/75 (mol/mol) mixture of poly(ethylene oxide) and resorcinol. DSC thermograms of these ternary complexes are presented in Fig. 15, and they reveal that there is only one composite melting event at 95 °C when the La^{3+} concentration is either 15 or 30 mol%. Since pure $LaCl_3(H_2O)_6$ melts at 95 °C, the composite melting endotherm at 95 °C in the two uppermost thermograms at 15 and 30 mol% La^{3+} in Fig. 15 probably contains contributions from a lanthanum-chloride-rich phase, in addition to liquidus melting. Heats of fusion for the liquidus endotherm in Table 2 support this claim via comparison of the 25/75 (mol/mol) binary mixture of PEO and resorcinol (i.e. 59–60 J/g), and the ternary which contains 15 mol% La^{3+} (i.e. 80–93 J/g). However, no endothermic response is observed between 30 and 120 °C for pure lanthanum chloride hexahydrate that was prepared from methanol at 35 °C and dried under vacuum at 45 °C for 24 h. This preparation for pure $LaCl_2(H_2O)_6$ was very similar to that for the ternary systems which contain lanthanum(III). Finally, the thermograms in Fig. 16 for PEO/resorcinol/Ce^{3+} ternary mixtures reveal that cerium chloride induces an approximate 16 °C decrease in liquidus melting at 105 °C and a 27 °C decrease in the PEO/resorcinol eutectic phase transition at 84 °C. An endotherm near 95 °C at higher Ce^{3+} concentrations in the three uppermost thermograms of Fig. 16 is attributed to a cerium–chloride-rich phase, which is consistent with the melting point of pure $CeCl_3(H_2O)_x$ at 97 °C. Most importantly, eutectic melting is not observed at

30 mol% Ce^{3+} in the uppermost thermogram of Fig. 16. From the viewpoint of eliminating the PEO/resorcinol eutectic phase transition at 84 °C, the efficiency of cerium is less than lanthanum, but greater than neodymium, terbium, and ytterbium.

A phenomenological explanation of the difference between lanthanum(III), cerium(III), terbium(III), and ytterbium(III) in these ternary mixtures with poly(ethylene oxide) and resorcinol can be traced to melting point depression of PEO in binary mixtures with each lanthanide complex. For example [59], PEO exhibits a significant melting endotherm at 58 °C in the presence of 25 mol% Tb^{3+} and 59 °C in the presence of 20 mol% Yb^{3+}, whereas PEO melting is absent when the concentration of $LaCl_3(H_2O)_6$ or $CeCl_3(H_2O)_x$ is between 16 and 20 mol%. Hence, there is greater tendency for lanthanum(III) or cerium(III) to interact with PEO in the molten state and disrupt eutectic solidification in ternary mixtures. Furthermore, (i) La^{3+} and Ce^{3+} are the 'lightest lanthanides', (ii) Tb^{3+} and Yb^{3+} are 'heavy lanthanides', (iii) lighter lanthanides might form complexes more exothermically if there is a change in the hydration sphere [60] as lattice waters are displaced by the ether oxygen of PEO, and (iv) La^{3+} (1.17 Å) and Ce^{3+} (1.15 Å) have larger ionic radii [60] than either Tb^{3+} (1.06 Å) or Yb^{3+} (1.01 Å). In particular, La^{3+}, which eliminates PEO/resorcinol eutectic melting at 84 °C most efficiently, has 22% more surface area than Tb^{3+} and 34% more surface area than Yb^{3+}, which might allow La^{3+} to accommodate more PEO repeat units in its first-shell coordination sphere with less steric hindrance. These facts could be invoked to explain why competitive interactions with poly(ethylene oxide) are more favourable in ternary

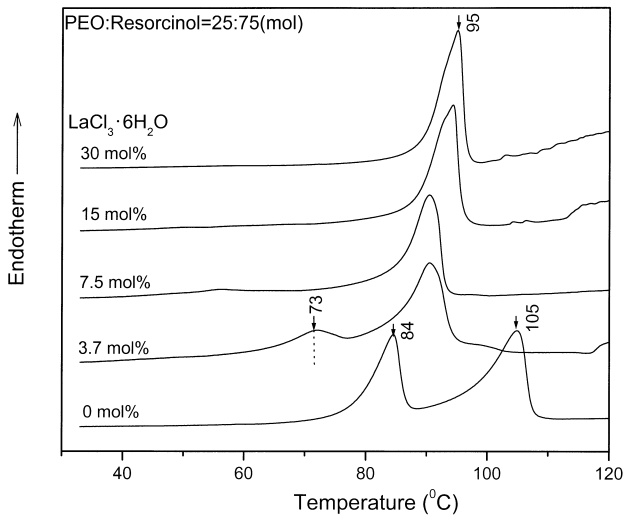

Fig. 15. DSC thermograms for ternary mixtures of poly(ethylene oxide), $\overline{M}_W = 2 \times 10^5$ Da, resorcinol, and lanthanum trichloride hexahydrate at a heating rate of 10 °C/min. The PEO/resorcinol molar ratio is 1:3 in each case, and the mole fraction of the low-molecular-weight lanthanide complex is indicated at the left of each thermogram. The dashed line at 73 °C identifies eutectic melting only in the ternary mixture which contains 3.7 mol% $LaCl_3(H_2O)_6$.

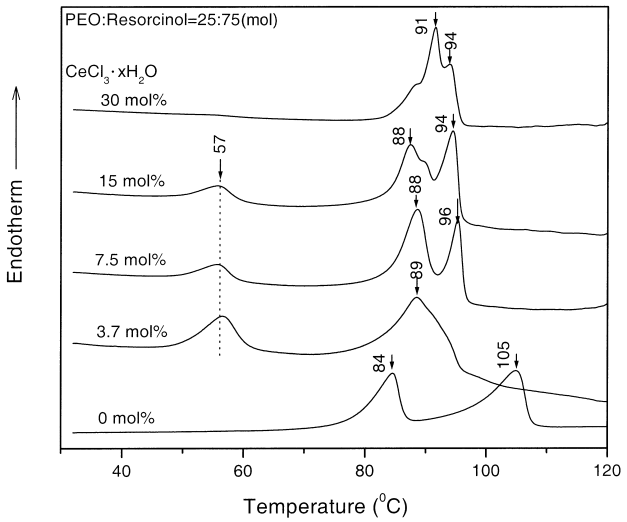

Fig. 16. DSC thermograms for ternary mixtures of poly(ethylene oxide), $\overline{M}_W = 2 \times 10^5$ Da, resorcinol, and cerium trichloride hydrate at a heating rate of 10 °C/min. The PEO/resorcinol molar ratio is 1:3 in each case, and the mole fraction of the low-molecular-weight lanthanide complex is indicated at the left of each thermogram. The dashed line at 57 °C identifies eutectic melting in ternary mixtures which contain 3.7, 7.5, and 15 mol% $CeCl_3(H_2O)_x$.

mixtures that contain lanthanum(III) or cerium(III), relative to either terbium(III) or ytterbium(III). Since neodymium(III) functions like terbium(III) and ytterbium(III), not like lanthanum(III) or cerium(III), it is not possible to invoke the abrupt and rather discontinuous changes in thermochemical properties which occur at the 'gadolinium break' [61] to identify lanthanide trichlorides that can compete with resorcinol, interact with poly(ethylene oxide), disrupt the PEO/resorcinol stoichiometric complex, and eliminate eutectic solidification upon cooling.

4. Conclusions

The solid state phase behavior of binary and ternary polymeric systems is correlated with the interaction-sensitive phenolic ^{13}C NMR signal of resorcinol near 160 ppm, because this resonance can detect the number and morphological nature of resorcinol-containing phases that coexist. In some cases, temperature-composition phase diagrams provide a phenomenological explanation of the fact that multiple resonances are observed for chemically equivalent ^{13}C sites in different molecular environments. The bi-eutectic phase behavior of poly(ethylene oxide) and resorcinol is not perturbed by polystyrene, but poly(2-vinylpyridine) disrupts the PEO/resorcinol stoichiometric complex and eliminates eutectic solidification. The phenolic carbon resonance of resorcinol can detect this small molecule aromatic (i) in the self-assembled pure-component crystalline state (i.e. phase γ) at 155 ppm, (ii) in a stoichiometric crystalline complex (i.e. phase β) with poly(ethylene oxide) at 158 ppm, (iii) in a homogeneous

amorphous mixture with poly(2-vinylpyridine) at 160 ppm, and (iv) in a disordered crystalline phase at 159 ppm, where defects are introduced by both poly(ethylene oxide) and poly(2-vinylpyridine). Competitive interactions among poly(ethylene oxide), resorcinol, and five different lanthanide trichloride hydrates depress one of the the PEO/resorcinol eutectic phase transitions from 84 to 74 °C (i.e. Yb^{3+}), 73 °C (i.e. Tb^{3+} and La^{3+}), 65 °C (i.e. Nd^{3+}), or 57 °C (i.e. Ce^{3+}). $LaCl_3(H_2O)_6$ eliminates eutectic solidification and the PEO/resorcinol stoichiometric complex when the concentration of La^{3+} is at least 15 mol%. Similar behavior is observed in the presence of 30 mol% cerium chloride, but cerium is less efficient than lanthanum. In contrast, eutectic solidification is not eliminated in ternary mixtures which contain as much as 30 mol% neodymium(III), terbium(III), or ytterbium(III). The lightest lanthanides, like La^{3+} and Ce^{3+}, with the largest ionic radii in the first-row of the f-block are most effective from the viewpoint of competing with resorcinol, interacting with poly(ethylene oxide), disrupting the PEO/resorcinol stoichiometric complex, and eliminating eutectic solidification.

Acknowledgements

The research described herein was supported by the National Science Foundation via Grant DMR-9902657. The ^{13}C solid state NMR experiments were performed at the Colorado State University NMR Center, located in the Department of Chemistry.

References

[1] Ciardelli F, Tsuchida E, Wöhrle D. Macromolecule–metal complexes. Berlin: Springer; 1996.
[2] Belfiore LA. Polymer 1986;27:80–90.
[3] Qin C, Pires ATN, Belfiore LA. Polym Commun 1990;31:177–82.
[4] Patwardhan AA, Belfiore LA. Polym Engng Sci 1988;28:916–25.
[5] Qin C, Pires ATN, Belfiore LA. Macromolecules 1991;24:666–70.
[6] Belfiore LA, Pires ATN, Wang Y, Graham H, Ueda E. Macromolecules 1992;25(5):1411–9.
[7] Belfiore LA, Graham H, Ueda E, Wang Y. Polym Int 1992;28(1):81–94.
[8] Belfiore LA, McCurdie MP, Ueda E. Macromolecules 1993;26(25):6908–17.
[9] Minier M, Berthier C, Gorecki W. J Phys 1984;45:739.
[10] James DB, Wetton RE, Brown DS. Polymer 1979;20:187.
[11] Marsh JS. Principles of phase diagrams. New York: McGraw-Hill; 1935. p. 87.
[12] Adamson AW. A textbook of physical chemistry. New York: Academic Press; 1973. p. 456.
[13] Myasnikova RM. Vysokomol Soedin 1977;A19:564.
[14] Myasnikova RM, Titova EF, Obolonkova ES. Polymer 1980;21:403.
[15] Belfiore LA, Lutz TJ, Cheng CM, Bronnimann CE. J Polym Sci, Polym Phys Ed 1990;28:1261–74.
[16] Cheng CM, Belfiore LA. Polym News 1990;15(2):39–49.
[17] Belfiore LA, Ueda E. Polymer 1992;33:3833–40.
[18] Point JJ, Damman P. Macromolecules 1992;25:1184.
[19] Paternostre L, Damman P, Dosiere M, Bourgaux C. Macromolecules 1996;29(6):2046–52.
[20] Iannelli P, Damman P, Dosiere M, Moulin JF. Macromolecules 1999;(7):2293–300.
[21] Spevacek J, Paternostre L, Damman P, Draye AC, Dosiere M. Macromolecules 1998;31(11):3612–6.
[22] Harris DJ, Bonagamba TJ, Hong M, Schmidt-Rohr K. Macromolecules 2000;33(9):3375–81.
[23] Tadokoro H. Structure of crystalline polymers. New York: Wiley-Interscience; 1979. p. 362 and 369.
[24] International Center for Diffraction Data, edited by the Joint Committee on Powder Diffraction Standards: Newton Square, PA.
[25] Smith P, Pennings AJ. J Mater Sci 1976;11:1450.
[26] Smith P, Alberda van Ekenstein GOR, Pennings AJ. Br Polym J 1977;9:258.
[27] Smith P, Pennings AJ. Polymer 1974;15:413.
[28] Wittmann JC, St John Manley R. J Polym Sci, Polym Phys Ed 1977;15:1089, 2277.
[29] Henley EJ, Seader JD. Equilibrium stage separation operations in chemical engineering. New York: Wiley; 1981. Chapter 3, p. 100, Figure 3.7.
[30] Hwang KKS, Hemker DJ, Cooper SL. Macromolecules 1984;17:307.
[31] Hwang KKS, Lin SB, Tsay SY, Cooper SL. Polymer 1984;25:947.
[32] Ke B, Sisko AW. J Polym Sci 1961;50:87.
[33] Mandelkern L. Crystallization of polymers. New York: McGraw-Hill; 1964. Chapter 4.
[34] Smith P, Koningsveld R, Schouteten CJH, Pennings AJ. Br Polym J 1980;12:215.
[35] Chadwick GA. Metallography of phase transformations. London: Butterworths; 1972. p. 107.
[36] Etter DE, Tucker PA, Wittenberg LJ. In: Thermal analysis, Vol. 2. Schwenker RF, Garn PD, editors. New York: Academic Press; 1969. p. 829–50.
[37] Gutt W, Majumdar AJ. In: Differential thermal analysis, Vol. 2. Mackenzie RC, editor. New York: Academic Press; 1972. Chapter 29.
[38] Belfiore LA. Polym Prepr 1987;28(2):114.
[39] Belfiore LA. Polym Prepr 1988;29(1):17.
[40] Belfiore LA. Polym Prepr 1988;29(1):430.
[41] Belfiore LA. Polym Prepr 1989;30(2):325.
[42] Ewing DF. Org Magn Reson 1979;12(9):499.
[43] Imashiro F, Maeda S, Takegoshi K, Terao T, Saika A. Chem Phys Lett 1982;92(6):642.
[44] Imashiro F, Maeda S, Takegoshi K, Terao T, Saika A. Chem Phys Lett 1983;99(2):189.
[45] Smith KL, Winslow AE, Petersen DE. Ind Engng Chem 1959;51:1361.
[46] Wind RA, Anthionio FE, Duijvestijn MJ, Smidt J, Trommel J, deVette GMC. J Magn Reson 1983;52:424.
[47] Stejskal EO, Schaefer J. J Magn Reson 1975;18:560.
[48] Paul DR, Barlow JW, Bernstein RE, Wahrmund DC. Polym Engng Sci 1978;18(16):1225.
[49] Greco R, Hopfenberg HB, Martuscelli E, Ragosta G, Demma G. Polym Engng Sci 1978;18(8):654.
[50] Twomey CJ, Chen SH. J Polym Sci, Polym Phys Ed 1991;29:859.
[51] Silva CRJ, Smith MJ. Electrochim Acta 1995;40(13–14):2389–92.
[52] Bekiari V, Lianos P, Judeinstein P. Chem Phys Lett 1999;307(5–6):310–6.
[53] Cruzpinto JJ, Silva MM, Smith MJ, Silva CRJ. J Therm Anal 1993;40(2):641–7.
[54] Puga MMS, Carlos LD, Abrantes TMA, Alcacer L. Electrochim Acta 1995;40(13–14):2383–7.
[55] Puga MMS, Carlos LD, Abrantes TMA, Alcacer L. Chem Mater 1995;7(12):2316–21.
[56] Carlos LD, Ferreira RAS, Bermudez VD, Molina C, Bueno LA, Ribeiro SJL. Phys Rev B 1999;60(14):10042–53.
[57] Silva MM, Smith MJ. Electrochim Acta 2000;45(8–9):1463–6.

[58] Bermudez VD, Carlos LD, Silva MM, Smith MJ. J Chem Phys 2000; 112(7):3293–313.
[59] Tang J, Lee, CKS, Belfiore LA. Effects of several lanthanide trichloride hydrates on the melting behavior and spherulitic superstructure of poly(ethylene oxide). J Polym Sci, Polym Phys Ed, under revision.
[60] Cotton FA, Wilkinson G, Murillo CA, Bochmann M. Advanced inorganic chemistry. New York: Wiley; 1999. p. 1109–17.
[61] Ashcroft SJ, Mortimer CT. Thermochemistry of transition metal complexes. London: Academic Press; 1970. p. 398–401.
[62] Das PK, Ruzmaikina I, Belfiore LA. J Polym Sci, Polym Phys Ed 2000;38:1931–8.